International Journal of Engineering Research & Technology (IJERT)
ISSN: 2278-0181
Vol. 5 Issue 11, November-2016

# Theoretical Design of Radiator using Heat Pipes

Archit Deshpande
Department of Mechanical Engineering
Smt. Kashibai Navale College of Engineering
Pune, India

Viraj Patil
Department of Mechanical Engineering
Pune Vidyarthi Griha's
College of Engineering and Technology
Pune, India

Rohit Patil
Department of Mechanical Engineering
Smt. Kashibai Navale College of Engineering
Pune, India

***Abstract* —A thermal radiator in an automobile has the function of preventing an engine from overheating and regulating engine temperature. Heat pipes are heat transfer devices with high thermal conductivity and with their use the radiator's frontal area can be made more compact or the heat transfer capacity of the radiator can be increased. The heat pipe radiator is designed to operate at conditions similar to that of a conventional radiator. Theoretical thermal calculations were carried out for verifying any improvement in its thermo-hydraulic performance. It was observed that for the same size of radiator the effective frontal area reduced by 37.17% and capacity reduced by 14.82%.**

***Keywords—Automobile radiator; Heat Pipe; Modified radaitor***

## I. NOMENCLATURE

| Symbol | Description | Unit |
|---|---|---|
| $A_c$ | Total Condenser Surface Area of Heat Pipes | m² |
| $A_e$ | Total Evaporator Surface Area of Heat Pipes | m² |
| $A_{ffa}$ | Air Side Free Flow Area | m² |
| $a_{sf}$ | Surface Area of Single Fin | m² |
| $A_f$ | Total Surface Area of Fin | m² |
| $A_{fa}$ | Air Side Frontal Area | m² |
| $A_p$ | Primary Surface Area | m² |
| $A_v$ | Cross-Sectional Area of Vapour Space | m² |
| $A_w$ | Cross-Sectional Area of Wick | m² |
| $B_o$ | Bond Number | -- |
| $C_{min}$ | Minimum Heat Capacity | kJ/K |
| $D_o$ | Outer diameter of heat pipe | m |
| $d_w$ | Wire Diameter | m |
| $\varepsilon$ | Porosity | -- |
| $\varepsilon_{overall}$ | Overall Effectiveness | -- |
| $f_l Re_l$ | Drag Coefficient | -- |
| $f_1, f_2, f_3$ | Entrainment Limit Factors | -- |
| g | Acceleration due to Gravity | m/s² |
| $h_a$ | Convective Heat Transfer Coefficient of Air | W/m²K |
| $h_w$ | Convective Heat Transfer Coefficient of Water | W/m²K |
| j | Colburn Factor | -- |
| K | Permeability of Wick | |
| $k_{Al}$ | Thermal Conductivity of Aluminium | W/mK |
| $k_{eff}$ | Effective Conductivity of Wick | W/mK |
| $k_w$ | Thermal Conductivity of Wick | W/mK |
| $k_{ca}$ | Air Side Contraction Factor | -- |
| $k_{cw}$ | Water Side Contraction Factor | -- |
| $k_{ea}$ | Air Side Expansion Factor | -- |
| $k_{ew}$ | Water Side Expansion Factor | -- |
| L | Latent Heat Of Vaporization of Working Fluid | kJ |
| $L_d$ | Total Length of Radiator | m |
| $l_c$ | Length of Condenser Section | m |
| $l_e$ | Length of Evaporator Section | m |
| $l_{eff}$ | Effective Length of Heat Pipe | m |
| $l_{hf}$ | Length of Hypotenuse of Fin | m |

International Journal of Engineering Research & Technology (IJERT)
ISSN: 2278-0181
Vol. 5 Issue 11, November-2016

| | | |
|---|---|---|
| $l_r$ | Radial Distance of Fin | m |
| $l_{tot}$ | Total Length of Heat Pipe | m |
| m | Parameter ‘M’ | $m^{-1}$ |
| $m_w$ | Mass flow rate of water as coolant | lpm |
| $\mu_v$ | Dynamic Viscosity of Vapour | $Ns/m^2$ |
| N | Number of Heat Pipes | -- |
| $N_f$ | Number of Waves per Fin | -- |
| $Nr_{row}$ | Number of Rows | -- |
| $NTU_h$ | Number of Transfer Units for Evaporator | -- |
| $NTU_c$ | Number of Transfer Units for Condenser | -- |
| $P_f$ | Fin pitch | m |
| $P_v$ | Vapour Pressure of Working Fluid | $N/m^2$ |
| $\Delta P_a$ | Air Side Pressure Drop | $N/m^2$ |
| $\Delta P_w$ | Water Side Pressure Drop | $N/m^2$ |
| $Q_{he}$ | Thermal Capacity of Radiator | kW |
| $r_c$ | Capillary Radius of Wick | m |
| $r_i$ | Inner Radius of Heat Pipe Wall | m |
| $r_{h,l}$ | Hydraulic Radius of Wick | m |
| $r_n$ | Nucleation Radius | m |
| $r_v$ | Radius of Vapour Space | m |
| $Re_a$ | Air Side Reynolds Number | -- |
| $\rho_l$ | Liquid Density | $kg/m^3$ |
| $\rho_l$ | Vapour Density | $kg/m^3$ |
| $\sigma_l$ | Surface Tension of Fluid | N/m |
| $s_d$ | Surface to Surface distance between the Heat Pipes | m |
| t | Thickness of heat pipe | m |
| $T_{ai}$ | Temperature of Air at Inlet | K |
| $T_{ao}$ | Temperature of Air at Outlet | K |
| $T_{wi}$ | Temperature of Water at Inlet | K |
| $T_{wo}$ | Temperature of Water at Outlet | K |
| $T_v$ | Saturation Temperature | K |
| $U_e$ | Overall Heat Transfer Coefficient at Evaporator Section | $W/m^2K$ |
| $U_c$ | Overall Heat Transfer Coefficient at Condenser Section | $W/m^2K$ |
| V | Velocity of air | m/s |
| $w_d$ | Width of Duct | m |
| $w_f$ | Width of Fin | m |
| $w_o$ | Outer Width of Heat Pipe | m |
| $X_l$ | Distance between the Heat Pipes along the direction of Air Flow | m |
| $X_t$ | Distance between the Heat Pipes across the direction of Air Flow | m |

## II. INTRODUCTION

A radiator is a type of heat exchanger and it has the functions of preventing engine from overheating. High temperatures in an engine can cause coolant to thin, engine parts to expand, lubrication to break down, and moving parts to be damaged. Most modern cars use aluminium radiators. These radiators are made by brazing thin aluminium fins to flattened aluminium tubes. Hot coolant flows across the flat core tubes and returns to the engine. The heat is transferred from the coolant to tube walls and then to the surrounding air via the fins mounted on the tubes.

Heat pipes are two-phase heat transfer devices with very high effective thermal conductance. Heat pipes utilize latent heat of vaporization to transfer heat energy from evaporator section to condenser section.

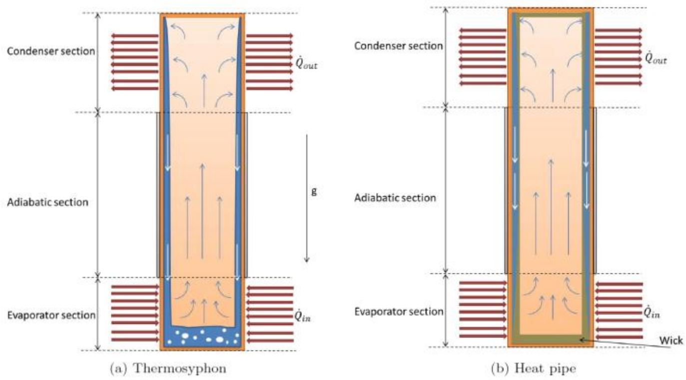


Fig. 1. Working of Heat Pipe

Applying heat to the evaporator section causes the liquid to vaporize. The vapour then flows from the hotter section due to the higher vapour pressure to the colder section of the heat pipe, where it is condensed. The liquid condensate then returns to the evaporator section from the condenser section under the assistance of gravity or capillary action of the wick. High heat transfer rates can be thus achieved with a small temperature difference between the evaporator and condenser sections.

Thermal devices like heat exchangers need to undergo continuous improvements which may imply subtle changes in the existing design to obtain maximum thermal efficiency or a complete change in the design altogether. In case of a radiator, an improvement in its thermal efficiency will help in reducing its size, thus allowing for more compact designs in automobiles. Such units would have lesser weight and frontal area which would help in making them more fuel efficient. '

## III. LITERATURE SURVEY

The operating characteristics of a heat pipe are governed by the thermodynamic properties of the working fluid. The heat transfer capacity of a heat pipe is directly proportional to the latent heat of vaporization of the fluid. Whereas other properties like density, viscosity and surface tension determine the flow characteristics of the working fluid. A.K. Mozumder et al [1] presented in 2010, The Performance of Heat pipes for Different Working Fluids and Fill ratios. Fill ratio is the volume occupied by the liquid to the total volume of the evaporator section. He compared the fluids- water, methanol and acetone for fill ratios of 35%, 55%, 85% and 100% in the heat pipe. Acetone showed minimum temperature difference at all fill ratios and also the highest heat transfer coefficients. The heat pipe performed best with water at 85% fill ratio and with acetone at 100% fill ratio.

Ammonia is another fluid which was widely used in cooling circuits for transferring heat. But for safety reasons, the toxicity of ammonia precludes its use in manned environments. An account of this was published by NASA [2] in a paper on Ammonia-charged Aluminium Heat Pipes with Extruded Wicks. It also highlighted that the purity of fluid used in a heat pipe had to be at least 99.99% and any traces of water in ammonia could lead to formation of hydrogen gas. To ensure that the heat pipe is leak proof, further importance was laid on X-ray verification of all welds and testing of the heat pipe at twice the maximum expected operating pressure.

Along with the material and the working fluid; the dimensions, wick structure and orientation of the heat pipe also have a major effect on the heat transfer limits. Qpediae Magazine [3] discusses the impact of orientation and wick structures on the thermal performance of a heat pipe. Grooved, mesh and sintered wicks were tested at different angles of inclination for the diameters 4 mm, 5 mm and 6 mm. The sintered wick heat pipe showed the least variation with change in the angle of inclination and was most effective when used against gravity. Grooved wick on the other hand performed best in gravity assisted situations. Also the wicks were tested for different loads and operating temperatures. As expected the heat pipes performed better at higher temperature.

While the research on the use of heat pipes to dissipate the heat generated by an automobile engine is limited, heat pipe heat exchangers have been in use for heat recovery applications for over a decade. Spirax Sarco [4] has successfully employed heat pipes in Energy Recovery Systems to cost effectively recovery energy from hot, corrosive and dirty exhausts. Traditional heat exchangers struggle to operate effectively in hostile environments due to build-up of materials and corrosion. Whereas the Heat Pipe Heat Exchanger (HPHE) is more robust and reliable as its isothermal pipe temperature avoids cold spots, reducing corrosion and the independent working of each pipe ensure minimal impact on performance during individual pipe failures. Also the system is flexible as individual pipes can be added or removed for precise optimization and maintenance. HPHE has several success stories like in Steel Casting Companies in Czech Republic or Ceramic Manufacturing Companies in India.

One of the few works suggesting the utilization of heat pipes in automobile radiators was presented by Yiding Cao et al [5] in a paper on An Automotive Radiator Employing Wickless Heat Pipes. It stated that HPR has higher effectiveness as the flow of air and the coolant is counter-flow as opposed to the cross-flow heat transfer in a conventional radiator. Leakages in a conventional radiator can be catastrophic, whereas in a HPR damage to an individual heat pipe will not affect the operation of other heat pipes. Thus HPR has high reliability. The thermal resistance of heat pipe is also negligible and the turbulent cross-flow heat transfer coefficient is much higher than the heat transfer coefficient of laminar flow in conventional radiator tubes. Thus, the overall heat transfer coefficient of HPR is very high. In a heat pipe radiator, the coolant flows through the lower coolant tank and not through tubes having very small cross-sectional area; hence the coolant pressure drop is much smaller.

## IV. DESIGN OF HEAT PIPE RADIATOR

The following input parameters were considered for the heat pipe.

Table I. Input Design Parameters

| Parameter | Value |
|---|---|
| $D_o$ | 12 mm |
| $L_e$ | 150 mm |
| $L_c$ | 250 mm |
| $L_d$ | 580 mm |
| $m_w$ | 110 lpm |
| $Nr_{row}$ | 4 |
| $P_f$ | 2.07 mm |
| $s_d$ | 2 mm |
| t | 0.25 mm |
| $t_f$ | 0.07 mm |
| $T_{ai}$ | 34ºC |
| $T_{wi}$ | 50ºC |
| V | 8 m/s |

Considering the working temperatures, the working fluid in the heat pipe was decided to be acetone. The material compatible with acetone was selected as aluminium. As the considered heat pipes were gravity assisted, there was no requirement of wick structure. The following heat flux limits were considered and the maximum permissible amount of heat capacity was calculated.

- Sonic limit ($Q_{sonic}$): Heat flux at which the vapour velocity reaches sonic limitation. The evaporator cannot respond to further decrease in pressure in condenser section so vapour flow is choked. It is calculated as in [8].

$$Q_{sonic} = 0.474 * A_v * L * (\rho_v * P_v)^{0.5} \tag{1}$$

- Viscous limit ($Q_{viscous}$): The heat flux for which the viscous forces are no longer dominant in the vapour section. It is calculated as in [8].

$$Q_{viscous} = \frac{A_v * r_v^2 * L * \rho_v * P_v}{16 * \mu_v * l_{eff}} \tag{2}$$

- Entrainment limit ($Q_{entrainment}$): The maximum heat flux after which the rising vapour starts to entrain the returning condensed fluid. It may lead to dry out of the evaporator section. It is calculated as in [6].

$$Q_{entrainment} = A_v * L * f_1 * f_2 * f_3 * \rho_v^{0.5} * (g * \sigma_l * (\rho_l - \rho_v))^{0.25} \tag{3}$$

- Capillary limit ($Q_{capillary}$): The heat transfer capacity based on ability of wick to pump the liquid back to the evaporator section. This limit depends on the wick permeability and properties of working fluid.

- Boiling limit ($Q_{boiling}$): Maximum heat flux after which nucleate boiling starts and bubble formation takes place in the evaporator section. The bubbles formed during evaporation may block the vapour flow. Bubble formation limits the heat transfer from the heat pipe wall to the working fluid which is by conduction only. It is calculated as in [6].

$$Q_{boiling} = 0.12 * L * \rho_v^{0.5} * (g * \sigma_l * (\rho_l - \rho_v))^{0.25} \tag{4}$$

$$Q_{max} = \min(Q_{sonic}, Q_{viscous}, Q_{entrainment}, Q_{boiling}) \tag{5}$$

*A. Geometrical Parameters*

a) Duct Side Geometrical Calculations: Staggered arrangement with an angle of ϕ = 30° was selected. Due to staggered arrangement of heat pipes, turbulent flow of air is developed in the radiator. Pressure drop is more in staggered case but characteristics related to more heat transfer due to arrangement compensates the pressure drop drawback. The formulae for staggered arrangement are as in[9]:

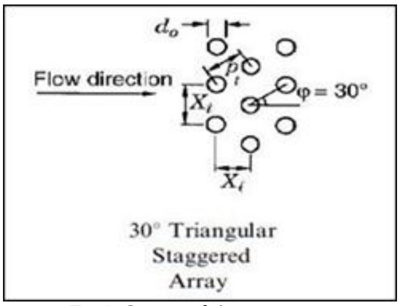


Fig.2. Staggered Arrangement

$$X_t = D_o + s_d \tag{6}$$

$$X_l = 0.866 * P_t \tag{7}$$

$$P_t = \sqrt{\frac{X_t}{2}^2 + \frac{X_l}{2}^2} \tag{8}$$

$$a = \frac{X_t - D_o - (X_t - D_o) * t_f * N_f}{2} \tag{9}$$

$$b = P_t - D_o - (X_t - D_o) * t_f * N_f \tag{10}$$

$$C_s = \min(2a, 2b) \tag{11}$$

Number of heat pipes in the whole heat exchanger is calculated as follows:

$$N = \frac{L_d}{X_t} * \left(\frac{\frac{W_d}{X_t} + 1}{2}\right) + \left(\frac{L_d}{X_t} - 1\right) * \left(\frac{\frac{W_d}{X_t} - 1}{2}\right) \tag{12}$$

Areas associated with Heat exchanger:

$$A_e = \left(3.14 * D_o * l_e + 2 * 3.14 * \left(\frac{D_o}{2}\right)^2\right) * N \tag{13}$$

$$A_c = \left(3.14 * D_o * l_c + 2 * 3.14 * \left(\frac{D_o}{2}\right)^2\right) * N \tag{14}$$

$$A_{fa} = L_d * l_c \tag{15}$$

$$A_{ffa} = \left(\left(\frac{L_d}{X_t} - 1\right) * C_s + X_t - D_o - (X_t - D_o) * t_f * N_f\right) * l_c \tag{16}$$

$$A_p = 3.14 * D_o * (l_c - l_c * t_f * N_f) * N + 2 * \left(L_d * W_d - 3.14 * D_o^2 * \frac{N}{4}\right) \tag{17}$$

b) Fin Geometrical Calculations: Rectangular flat fins were selected as they were most suitable in combination with the circular heat pipes. Also fin surface area is increased due to rectangular fins as compared to circular fins which assist in increasing heat transfer to the surrounding air. It is calculated as in [9].

International Journal of Engineering Research & Technology (IJERT)
ISSN: 2278-0181
Vol. 5 Issue 11, November-2016

$$A_f = 2 * \left(L_d * W_d - 3.14 * 0.25 * D_o{}^2 * N\right) * l_c * N_f + 2 * L_d * l_c * t_f * N_f \quad (18)$$

$$N_f = \frac{1}{P_f} \quad (19)$$

$$D_e = \sqrt{\frac{4 * L_d * W_d}{3.14 * N}} \quad (20)$$

$$P_f = t_f + s_d \quad (21)$$

$$l_r = \left(\frac{D_e - D_o}{2}\right) + \frac{t_f}{2} \quad (22)$$

$$D_c = D_o + 2 * t_f \quad (23)$$

*B. Thermal Calculations*

a) Fin Thermal Calculations:

I. Fin Efficiency

$$m = \sqrt{\frac{2 * h_a}{k_{Al} * t_f}} \quad (24)$$

$$n_1 = e^{(0.13 * m * l_r - 1.3683)} \quad (25)$$

$$Z = m * l_r * \left(\frac{D_e}{D_o}\right)^{n_1} \quad (26)$$

$$\eta_f = \frac{\tanh Z}{Z} \quad (27)$$

II. Fin Effectiveness

$$\varepsilon_o = 1 - \left[\frac{A_f * (1 - \eta_f)}{A_f + A_{c,tot}}\right] \quad (28)$$

b) Thermal Resistances in Radiator: Resistances were calculated based on the path of heat transfer from water on evaporator side to air on condenser side. Axial resistance of heat pipe wall $R_{w,a}$ was taken as infinite whereas axial resistance of vapour space $R_{v,a}$ was considered negligible. It is calculated as in [8].

- Air side convective resistance

$$R_a = 1/\left[\varepsilon_o * h_a * (A_f + A_p)\right] \quad (29)$$

- Water side convective resistance

$$R_w = 1/(h_w * A_e) \quad (30)$$

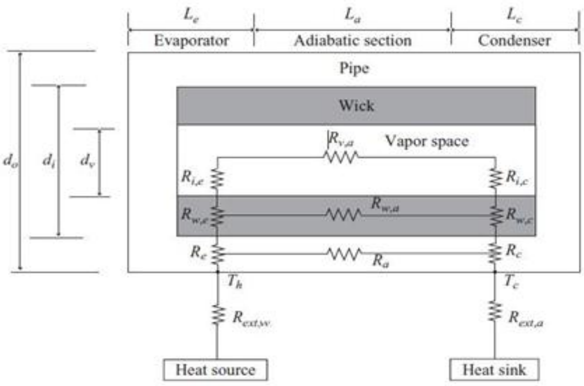


Fig.3. Resistances in Heat Pipe

- Evaporator side conductive resistance

$$R_e = \frac{\ln\left[\frac{D_o}{D_i}\right]}{[2 * \pi * k_{Al} * l_e * N]} \quad (31)$$

- Condenser side conductive resistance

$$R_c = \frac{\ln\left[\frac{D_o}{D_i}\right]}{[2 * \pi * k_{Al} * l_c * N]} \quad (32)$$

- Evaporator internal resistance

$$h_{el} = A = \frac{4}{3} * \left(\frac{\rho_l{}^2 * 9.81 * L * k_l{}^3}{4 * \mu_l * l_e * (T_{we} - T_{sat})}\right) \quad (33)$$

$$R_{ch} = 1/(h_{el} * A_e) \quad (34)$$

- Condenser internal resistance

$$h_{cl} = A = \frac{4}{3} * \left(\frac{\rho_l{}^2 * 9.81 * L * k_l{}^3}{4 * \mu_l * l_c * (T_{wc} - T_{sat})}\right) \quad (35)$$

$$R_{eh} = 1/(h_{cl} * A_c) \quad (36)$$

- Total resistance in evaporator and condenser

$$R_{eva} = (R_w + R_e + R_{eh}) \quad (37)$$

$$R_{con} = (R_a + R_c + R_{ch}) \quad (38)$$

c) Thermal Calculations: Thermal calculations for the heat pipe radiator were performed by using e-NTU method. It is calculated as in [9].

- Water side Convective heat transfer coefficient

$$h_w = \frac{Nu_w * k_w}{L_{ch}} \quad (39)$$

- Air side Convective heat transfer coefficient

$$h_a = j * G_a * C_{pa} * Pr^{\left(-\frac{2}{3}\right)} \quad (40)$$

- Colburn factor

$$c_3 = -0.361 - \frac{0.042 * N_{row}}{\ln(Re_a)} + 0.158 * \ln\left(N_{row} * \left(\frac{p_f}{D_c}\right)^{0.41}\right) \quad (41)$$

$$c_4 = -1.224 - \frac{0.076 * \left(\frac{X_l}{D_h}\right)^{0.41}}{\ln(Re_a)} \quad (42)$$

$$c_5 = -0.083 + \frac{0.058 * N_{row}}{\ln(Re_a)} \quad (43)$$

$$c_6 = -5.735 + 1.21 * \ln\left(\frac{Re_a}{N_{row}}\right) \quad (44)$$

$$j = 0.086 * Re_a^{c_3} * N_{row}^{c_4} * \left(\frac{p_f}{D_c}\right)^{c_5} * \left(\frac{p_f}{D_h}\right)^{c_6} * \left(\frac{p_f}{X_t}\right)^{-0.93} \quad (45)$$

The following are calculated as in [10].

- Overall heat transfer coefficient

$$U_e = \frac{1}{[R_{eva} * A_e]} \quad (46)$$

$$U_c = \frac{1}{[R_{con} * A_c]} \quad (47)$$

- Effectiveness

$$Ntu_h = \frac{U_e * A_e}{C_w} \quad (48)$$

$$Ntu_c = \frac{U_c * A_c}{C_a} \quad (49)$$

$$\varepsilon_h = 1 - e^{(-Ntu_h)} \quad (50)$$

$$\varepsilon_c = 1 - e^{(-Ntu_c)} \quad (51)$$

$$\varepsilon_{hn} = 1 - (1 - \varepsilon_h)^{N_{row}} \quad (52)$$

$$\varepsilon_{cn} = 1 - (1 - \varepsilon_c)^{N_{row}} \quad (53)$$

$$C_{str} = \frac{C_a}{C_w} \quad (54)$$

$$\varepsilon_{overall} = \frac{1}{\left(\frac{1}{\varepsilon_{cn}} + \frac{C_{str}}{\varepsilon_{hn}}\right)} \quad (55)$$

- Thermal capacity

$$Q_{HE} = \varepsilon_{overall} * C_{min} * (T_{wi} - T_{ai}) \quad (56)$$

- Water outlet temperature

$$T_{wo} = T_{wi} - \frac{\varepsilon_{overall} * C_{min} * (T_{wi} - T_{ai})}{C_w} \quad (57)$$

- Air outlet temperature

$$T_{ao} = \frac{\varepsilon_{overall} * C_{min} * (T_{wi} - T_{ai})}{C_a} - T_{ai} \quad (58)$$

## C. Pressure Drop

The following are calculated as in [9].

### a) Air Side Pressure Drop

- Friction factor:

$$c_7 = -0.764 + \left(0.739 * \left(\frac{X_t}{X_l}\right)\right) + \left(0.177 * \left(\frac{P_f}{D_c}\right)\right) - \left(\frac{0.00758}{N_{row}}\right) \quad (59)$$

$$c_8 = -15.689 + \left(\frac{64.021}{\ln(Re_a)}\right) \quad (60)$$

$$c_9 = 1.696 - \left(\frac{15.695}{\ln(Re_a)}\right) \quad (61)$$

$$f_a = 0.0267 * (Re_a^{c_7}) * \left(\left(\frac{X_t}{X_l}\right)^{c_8}\right) * \left(\left(\frac{P_f}{D_c}\right)^{c_9}\right) \quad (62)$$

- Pressure Drop

$$\Delta P_a = \frac{G_a^2}{2 * g_c * \rho_{ai}} * \left(1 - \sigma_a^2 + k_{ca} + \left(2 * \left(\frac{\rho_{ai}}{\rho_{ao}} - 1\right)\right) + \left(f_a * 4 * \frac{W_d}{D_h} * \rho_{ai} * \frac{1}{\rho_m}\right) - (1 - \sigma_a^2 - k_{ea}) * \frac{\rho_{ai}}{\rho_{ao}}\right) \quad (63)$$

### b) Water Side Pressure Drop

- Friction Factor

$$\alpha_{str} = \frac{H_d}{W_d} \quad (64)$$

$$f_w = 0.0791 * Re_w^{-0.25} * (1.0875 - 0.1125 * \alpha_{str}) \quad (65)$$

- Pressure Drop

$$\sigma_w = \frac{A_{ffw}}{A_1} \quad (66)$$

$$\Delta P_w = \frac{G_a^2}{2 * g_c * \rho_{ai}} * \left(1 - \sigma_w^2 + k_{cw} + f_w * \frac{L_d}{R_{hw}} - (1 - \sigma_w^2 - k_{ew})\right) \quad (67)$$

International Journal of Engineering Research & Technology (IJERT)
ISSN: 2278-0181
Vol. 5 Issue 11, November-2016

## V. RESULTS AND DISCUSSION

Maximum heat flux limit: The minimum value among the heat transfer limits of heat pipe was considered as the maximum value for designing heat pipe. The maximum heat transfer limit was $Q_{max} = Q_{entrainment}$ = 405.7W. This limit, if exceeded, would result in the failure of heat pipe.

Effect on dimensions of radiator: Due to the reduction in condenser section area of modified heat pipe radiator, the net frontal area reduces by 37.17% as compared to conventional radiator. The width of the radiator increases by 166.27%. This is because of the staggered arrangement of the pipes in the heat pipe radiator as opposed to inline (parallel) arrangement in the conventional radiator. The numbers of heat pipes are greater than the number of tubes in the conventional radiator, hence a staggered arrangement proves to be more effective than the inline arrangement.

Even though the size of the radiator is reduced, its weight increases due to the inclusion of additional working fluid inside the heat pipes. Also the increase in number of heat pipes contributes to the increase in weight of the radiator. This increase in weight is accompanied by increase in cost due to the requirement of additional materials.

Effect on Heat Capacity: Despite having lesser frontal area, the capacity of the heat pipe radiator is lesser than that of the conventional radiator by 14.82%. This is because there is an increase of 53.67% in the effectiveness of the radiator. As the capacity of the radiator is reduced, the exit temperature of the water is increased. This signifies lesser amount of heat transfer from the coolant to the heat pipes. But the exit temperature of air is higher due to prolonged flow through the staggered arrangement of heat pipes.

## VI. CONCLUSION

From the above study we conclude that:

- A heat pipe radiator reduces the size of the frontal area for almost the same thermal capacity.
- There is also an increase in other factors like effectiveness and air and water side heat transfer coefficients.
- But all these positive changes are at the expense of an increase in width of the radiator.
- This in turn increases number of heat pipes and also the total weight of the radiator due to inclusion of additional fluids inside them.
- The increase in weight is accompanied by increase in cost due to requirement of additional materials.

## REFERENCES

[1] A.K. Mozumder, A.F. Akon, M.S.H. Chowdhury and S.C. Banik, “Performance of Heat Pipe for Different Working Fluids and Fill Ratios”, December 2010, Journal of Mechanical Engineering, The Institution of Engineers, Bangladesh.
[2] NASA, “Ammonia-Charged Aluminium Heat Pipes with Extruded Wicks”, Preferred Reliability Practices, No: PD-ED-1209.
[3] “The Impact of Orientation on a Heat Pipe’s Performance with Different Wick Structures”, QpediaeMagazine, 2013.
[4] SpiraxSarco, Heat Pipe Heat Exchanger - An Energy Recovery Solution, Heat transfer solutions.
[5] Yiding Cao and KhokiatKengskool, “An Automotive Radiator Employing Wickless Heat Pipes”, Florida International University, Miami.
[6] Heat Pipes – Theory, Design and Applications, Fifth Edition by David Reay and Peter Kew.
[7] Heat Pipe Design and Technology by BahmanZohuri.
[8] Thermal Design: Heat Sinks, Thermoelectrics, Heat Pipes, Compact Heat Exchangers, and Solar Cells by Ho Sung Lee, pp. 180-235
[9] Fundamentals of Heat Exchanger Design by Ramesh K. Shah and Dusan P. Sekulic.
[10] Heat Pipe Science and Technology by Amir Faghri.